

ENVIRONMENTAL AND THERMAL PROTECTION OF HIGH Nb-CONTAINING GAMMA TITANIUM ALUMINIDES

Christoph Leyens and Reinhold Braun

German Aerospace Center (DLR), Institute of Materials Research
51170 Cologne, Germany

Keywords: gamma titanium aluminides, coatings, Ti-Al-Cr-Y-N, oxidation, thermal barrier coating, magnetron sputtering, EB-PVD

Abstract

For use at elevated temperatures, γ -TiAl alloys require protection against the oxidizing environment. In the present study nitride coatings based on Ti-Al-Cr-Y-N, either monolithically grown or with superlattice structure, as well as metallic Ti-Al-Cr and Ti-Al-Ag coatings were tested in air at 750°C up to 3000 h. Particularly the nitride coatings provided excellent oxidation protection under isothermal and cyclic conditions. Microstructure investigations revealed formation of protective oxide scales and long-term stability of the nitrides. Moreover, thermal barrier coatings deposited by EB-PVD demonstrated very promising lifetime results at 850 and 900°C, while at 950°C rapid oxidation of the Ti-45Al-8Nb base alloy led to early spallation of the ceramic top coating. Oxidation of the base alloy at all temperatures leads to a fairly complex setup of the oxide scale. Adjacent to the metal/oxide interface nitrides form that might affect oxide scale formation.

Introduction

Engineering titanium aluminide alloys based on γ -TiAl have convincingly demonstrated that they can meet the requirements for automotive combustion engines (exhaust valves and turbocharger wheels) as well as for aero engines (compressor and turbine blades) [1, 2]. While titanium aluminides are already in use in automotive applications, in some cases the risk and cost issues of γ -TiAl implementation into aero engines are seen higher than tolerable in current engine development programs [2], thus preventing these alloys from aero engine application. Nevertheless, the potential of titanium aluminides is indisputable [3] and has spurred R&D activities world-wide. Among others, alloy development aims at increased temperature capabilities up to temperatures in excess of 900°C. Although γ -TiAl alloys possess better intrinsic resistance against environmental attack than, e.g., conventional titanium alloys, protective coatings will be required for both, environmental protection and thermal insulation of the structural material.

In the present paper, a new approach is described to improve the environmental resistance of titanium aluminides by nitride overlay coatings produced by combined cathodic arc/unbalanced magnetron sputtering as well as metallic overlay coatings produced by conventional magnetron sputtering. Thermal barrier coatings (TBCs), typically applied to nickel-base superalloys, were also applied to a γ -TiAl alloy and a first assessment of TBC durability in the temperature range between 850 and 950°C was made.

Experimental

Extruded gamma titanium aluminide alloy Ti-45Al-8Nb provided by GKSS in Germany was used as substrate material; Ti-48Al-2Cr-2Nb was included as a reference material. Specimen geometries were 15mm in diameter and 1mm in thickness; the surfaces were ground with SiC paper up to 2500 grit. Prior to coating deposition specimens were cleaned ultrasonically using an industrial cleaning procedure.

An industrially sized HTC 100-4 [4] coating unit installed at Sheffield Hallam University was used to deposit Ti-Al-Cr-(Y)-N coatings. Prior to coating deposition, the substrate surface was subjected to an intensive metal ion bombardment. In this step, Cr^+ ions (average charge-state of 2.1) are generated from steered arc discharge sustained on one Cr target. The ions are then accelerated to the substrate by the applied high bias voltage ($U_b = -1200\text{V}$). The energy acquired by the metal ions ($E_i \sim 2.5 \text{ keV}$), is sufficient for intensive sputter cleaning of the substrate surface and more importantly to produce low energy implantation combined with radiation damage enhanced diffusion [5, 6]. Two types of coatings were produced: monolithically grown TiAlCrYN (nitride-1) and TiAlYN/CrN (nitride-2) coatings. The microstructure of the TiAlCrYN and the TiAlYN/CrN coatings is single phase NaCl, whilst the TiAlYN/CrN coating exhibits a superlattice structure consisting of alternating layers of Y-free TiAlN, Y-rich TiAlYN, and CrN. Details on the coating process are given in [7]. After nitride coating deposition the coating process was concluded by deposition of a thin oxy-nitride layer as described elsewhere [8]. For comparison, metallic Ti-Al-Cr and Ti-Al-Ag coatings produced by magnetron sputtering in a laboratory coater [9, 10] were included in this study.

Thermal barrier coatings (7wt.% partially yttria stabilized zirconia (PYSZ)) were deposited using a 150kW electron-beam physical vapor deposition (EB-PVD) coater installed at DLR; coating thickness was 190 μm . Prior to thermal barrier coating deposition the substrates were pre-oxidized to form an alumina scale; two different pre-oxidation procedures were used, the resulting thermal barrier coatings are designated TBC-1 and TBC-2.

Quasi-isothermal oxidation tests were performed in box furnaces at 750°C in air. The specimens were placed in alumina crucibles covered with alumina lids to collect any spalled oxide during cooling of the specimens. Specimens were weighed and visually inspected before exposure and once every week up to a total exposure time of 3000 h. Cyclic oxidation tests were carried out in automated rigs in air at 750°C, and thermal barrier coatings were tested at 850, 900 and 950°C in air up to 1000 cycles. One cycle consisted of 1 h at temperature and 10 min cooling down to 70°C. Post-oxidation analysis was performed using a LEO Gemini FEG-SEM with an Oxford EDS detector attached.

Results and Discussion

Quasi-isothermal and cyclic oxidation behavior of nitride coatings on gamma TiAl

Quasi-isothermal oxidation tests in air at 750°C reveal significant reduction in mass gain provided by both types of nitride coatings (Fig. 1). Oxidation resistance of Ti-48-2-2 is improved by at least one order of magnitude, while for inherently more resistant Ti-45-8 improvement by a factor of four can be achieved. While both nitride coatings have demonstrated long-term stability at 750°C, the monolithically grown TiAlCrYN (nitride-1) appears to have superior oxidation resistance compared to the superlattice (nitride-2) counterpart. Notably, oxidation resistance of the nitride-2 coating was extremely high during the initial stages of oxidation, however, mass gain increased more rapidly after about 200h of

exposure. The reason for this excellent initial oxidation resistance has not been explored but is subject of current research. In all cases adhesion of the oxide scale was excellent, no spall was found in the alumina crucibles.

The cyclic air oxidation behavior at 750°C of Ti-45-8 and Ti-48-2-2 coated with the nitride-2 as well as metallic overlay coatings is shown in Fig. 2. While high Nb-containing Ti-45Al-8Nb demonstrated already better oxidation resistance than reference alloy Ti-48-2-2, the metallic Ti-Al-Cr and Ti-Al-Ag coatings further reduce mass gain due to less oxygen uptake and oxide scale formation. Notably, the metallic coatings initially follow similar mass gain kinetics as the uncoated material, however, the rate is significantly reduced after about 100 1-h cycles thermal exposure at 750°C indicating protective oxide scale formation on the coated samples while oxidation of the uncoated counterparts continues with a comparably high oxidation rate. For the Ag-containing metallic coating spallation of part of the coating was observed after 700 cycles leading to a sudden mass loss. Obviously, best oxidation protection was provided by the nitride-2 coatings that demonstrated extremely low mass gain during the initial stages of oxidation (up to 200 h, see also Fig. 1) and low growth rates up to 1000 1-h cycles, resulting in mass gain of the order of one magnitude lower than for uncoated Ti-48-2-2. Oxidation protection of the nitride-2 coatings was obviously not affected by the substrate alloy chemistry, suggesting sufficient diffusional stability over the test duration.

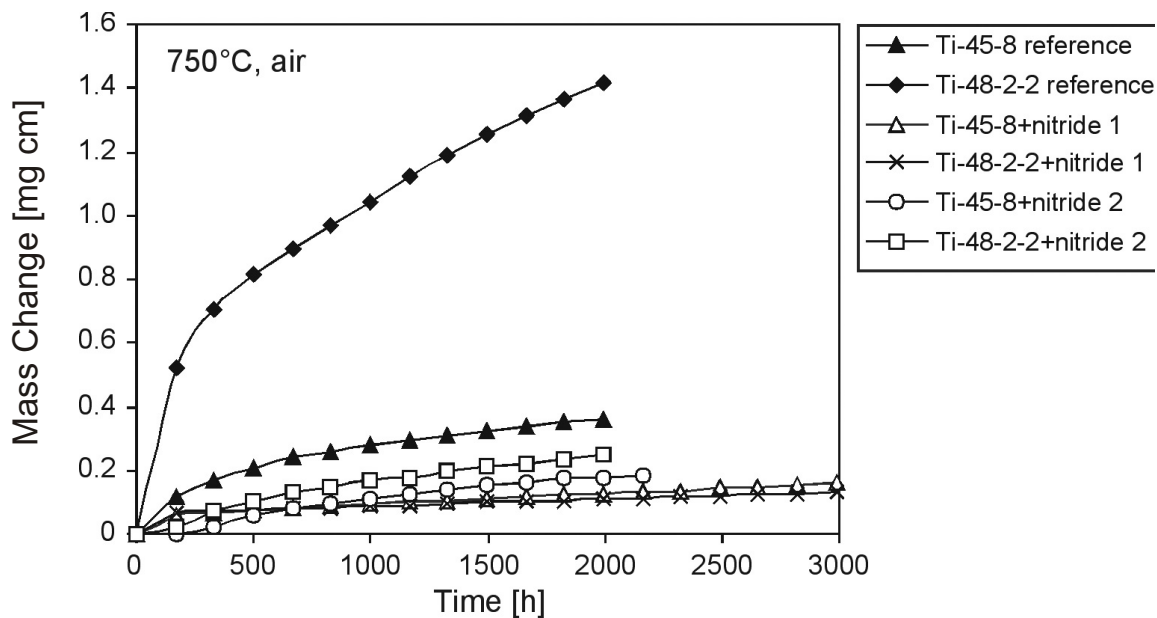


Figure 1: Quasi-isothermal oxidation behavior of reference and coated gamma titanium aluminide alloys.

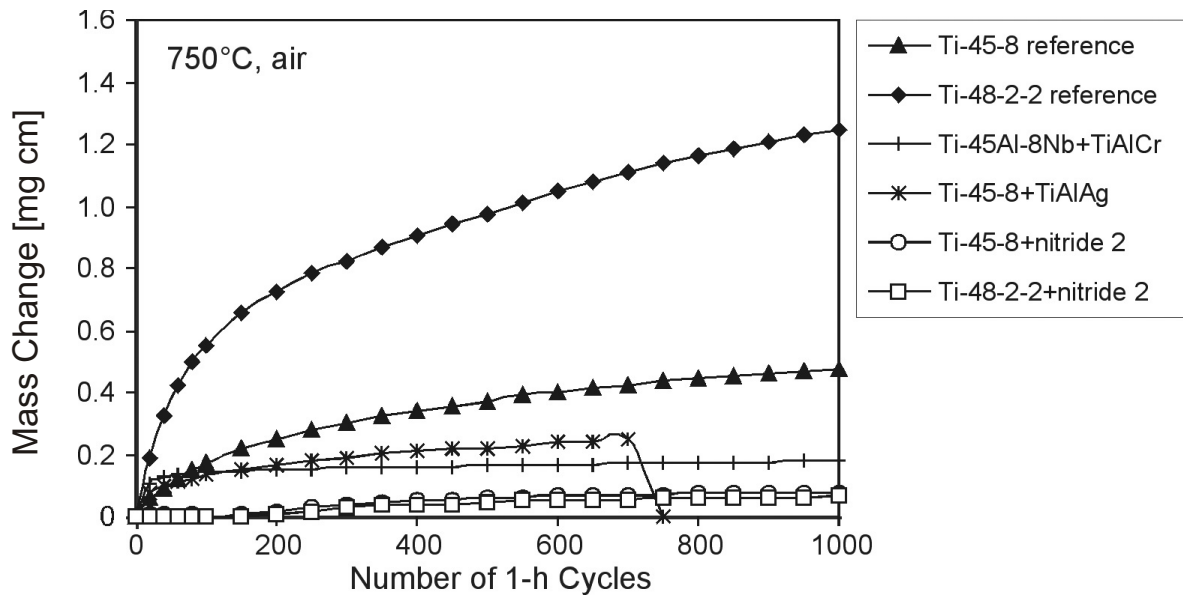


Figure 2: Cyclic oxidation behavior of reference and coated gamma titanium aluminide alloys Ti-48-2-2 and Ti-45-8.

Post-oxidation testing microstructure analysis

Scanning electron microscopy revealed the formation of dense oxides on the surfaces of γ -TiAl specimens coated with nitride-2 (Fig. 3). The coarse particles might be chromia, whereas the columnar ones were rutile. Needle-shaped crystals were also observed, but they were not the dominant oxide. Figure 4a shows the cross-section of an oxidized Ti-45-8 specimen, exhibiting dense oxides at the top of the scale, an adjacent porous oxide layer, the remnant nitride coating, a base layer, and an interface between nitride coating and substrate. Results of an EDX analysis of cross-section are plotted in Figure 4b. The concentration profiles indicate an increase in chromium at the top of the oxide scale, whereas titanium and aluminum are depleted. The porous layer beneath these compact oxides consist of a mixture of Cr_2O_3 , Al_2O_3 , and TiO_2 . It appears that approximately half of the nitride coating was oxidized during exposure at 750°C for 2200 h. Yttrium was neither detected in the oxide scale nor in the remaining nitride coating.

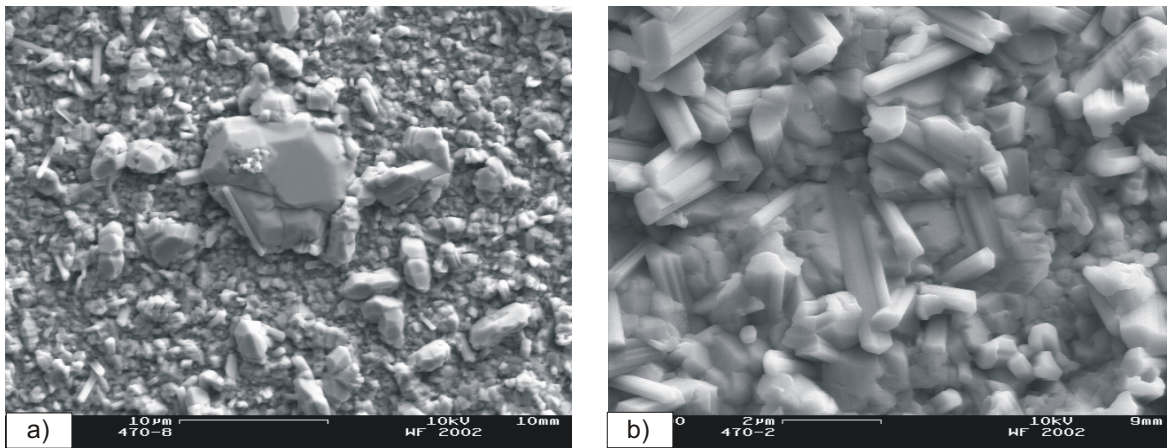


Figure 3: Top view scanning electron micrographs of nitride-2 coatings deposited onto a) Ti-45-8 and b) Ti-48-2-2 substrates. Specimens were isothermally oxidized in air at 750°C for 2200 h and 2000 h, respectively.

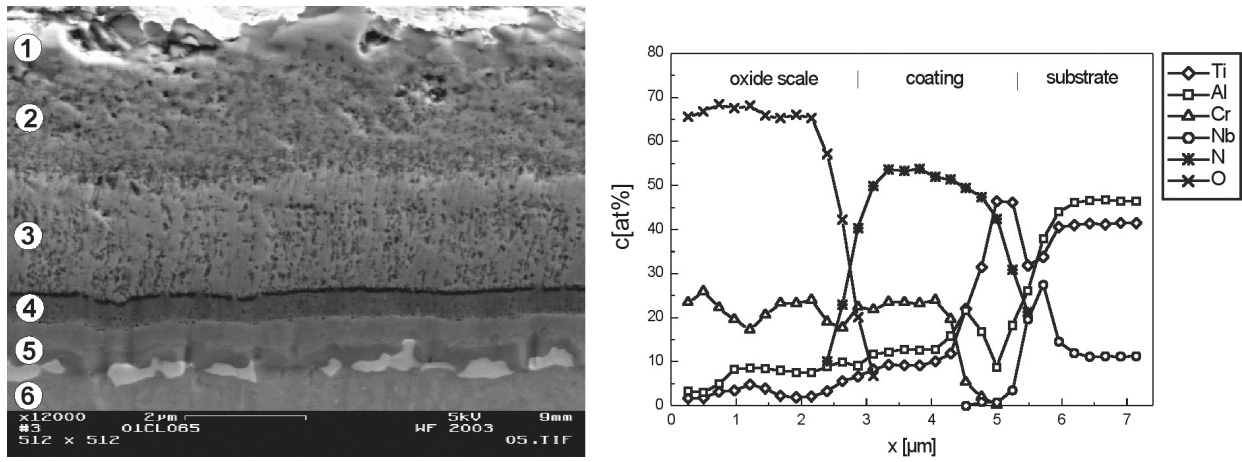


Figure 4: Scanning electron micrograph and EDX analysis of a Ti-45-8 specimen coated with nitride-2 which was oxidized for 2200 h at 750°C, showing a cross section view and the elemental profiles of the oxide scale (dense (1) and porous (2) part), nitride coating (3), base layer (4) and substrate (6). Clearly a transition zone (5) forms between the coating and the substrate.

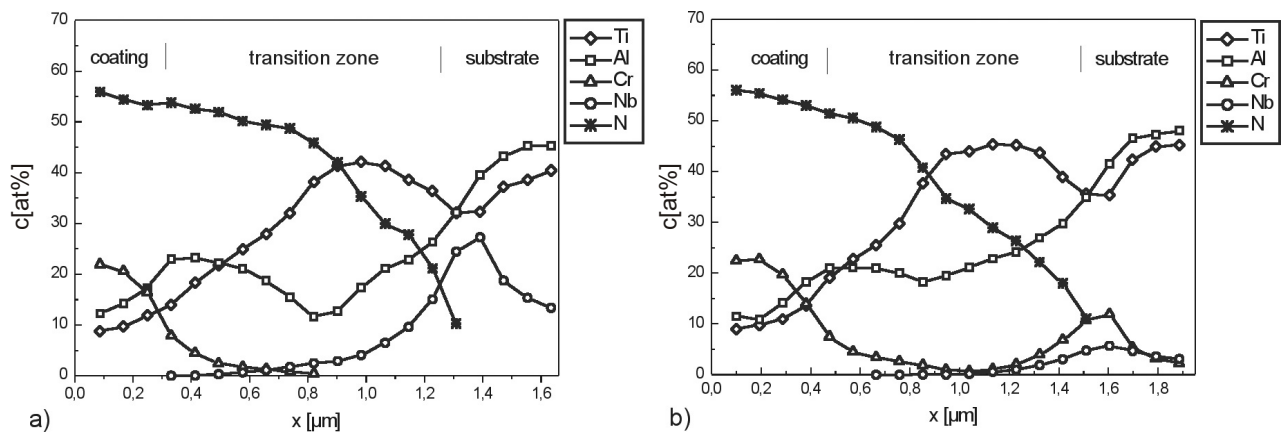


Figure 5: EDX analysis of Ti-45-8 (a) and a Ti-48-2-2 (b) specimens coated with nitride-2, which were oxidized at 750° C for 2200 h and 2000 h, respectively, showing elemental profiles across the transition zone between coating and substrate.

EDX analysis revealed a transition zone between nitride coating and substrate formed by interdiffusion of nitrogen and the alloying elements Ti and Al (Fig. 5). Across the interface, nitrogen decreased, whereas titanium was enriched. The aluminum profile exhibited a minimum being more pronounced with Ti-45-8 (a) than with Ti-48-2-2 (b). Diffusion of chromium and niobium was low through the transition zone. In the metal subsurface intermetallic phases precipitated rich in the alloying elements Nb and Nb + Cr for the substrates Ti-45-8 and Ti-48-2-2, respectively. The high concentration of Ti in the transition zone might be associated with formation of titanium nitride. As suggested by EDX point analysis, the titanium nitride layer consisted of two different nitrides, TiN and Ti₂AlN adjacent to the coating and the substrate, respectively (Table 1). The concentration minimum of aluminum in the transition zone supported the formation of TiN when the amount of nitrogen was high enough adjoining the nitride coating. The enrichment of aluminum in the upper part of the transition zone might be related to different compositions of the base layer and the nitride coating or to the formation of TiN causing an enhanced outward diffusion of aluminum.

Table 1. Results of EDX point analysis at different locations in the transition region between nitride coating and substrate for oxidized Ti-45-8 and Ti-48-2-2 specimens (in at%)

	Ti	Al	Cr	Nb	Y	N	Fe
Ti-45-8 coated with nitride-2; oxidized at 750°C for 2200 h							
nitride coating	10.3	11.3	25.2			53.1	
base layer	23.5	21.3	4.3	0.4		50.5	
upper nitride layer	45.7	9.2	0.6	0.9		43.7	
lower nitride layer	48.4	19.6		3.1		28.9	
bright phase	36.6	36.5		26.9			
Matrix	42.1	46.6		11.2			
Ti-48-2-2 coated with nitride-2; oxidized at 750°C for 2000 h							
nitride coating	8.8	10.4	24.0			56.8	
base layer	23.3	19.9	3.8	0.3		52.8	
nitride layer	45.8	22.3	0.6	0.5		30.8	
bright phase	36.7	40.6	13.3	5.5			2.6
Matrix	48.2	47.4	2.2	2.1			

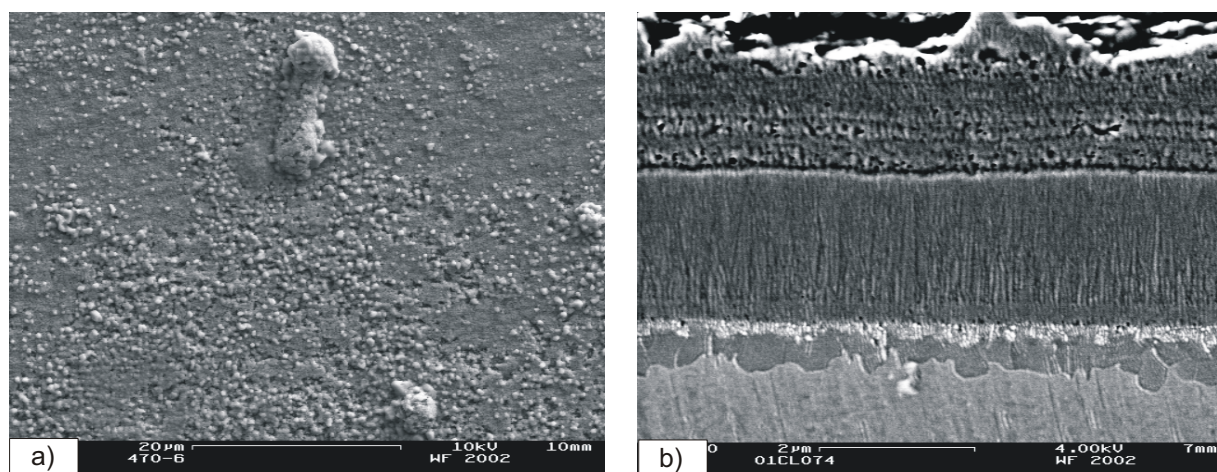


Figure 6: Scanning electron micrograph of a Ti-45-8 specimen coated with nitride-1, which was oxidized 3000 h at 750°C, showing a top view of the oxide scale (a) and a cross section through the oxide scale, nitride coating and substrate (b).

The oxidized surface of the nitride-1 coating was very porous, as illustrated by scanning electron micrographs of the surface and the cross-section of a specimen oxidized for 3000 h at 750°C (Fig. 6). Only few agglomerations of oxides were observed. The porous oxide scale consisting of a mixture of oxides revealed a layered structure with alternating enrichment in Al_2O_3 and TiO_2 (Fig. 7a). Chromium and yttrium were also detected in the oxide scale, however, at relatively small levels ($\text{Cr} \leq 1.5$ at%, $\text{Y} \leq 0.8$ at%). Yttrium was not found in the outer part of the oxide scale. Again, oxygen was not detected in and beyond the remaining nitride coating which exhibited a columnar grain morphology. Scanning electron micrographs revealed a base layer at the lower end of the nitride coating. The initial composition of this layer was different from that of the protective coating. However, the measurement of different concentration levels was impeded by interdiffusion between the nitride layer and the substrate, as shown in Fig. 7b. In the transition zone, the titanium concentration increased whereas

aluminum was depleted. The concentration of nitrogen decreased towards the substrate revealing an intermediate plateau near the coating layer. The enrichment of titanium was related to the formation of titanium nitride. Because of the high level plateau in nitrogen concomitant with a very low aluminum concentration, this part of the transition zone consisted of TiN. With decreasing nitrogen and increasing aluminum content, Ti_2AlN might be formed adjacent to the substrate. The titanium nitride layer exhibited a fine grain size as demonstrated by scanning electron micrographs of ion-beam etched cross-sections (Fig. 8). The formation of two different titanium nitrides was less pronounced in the transition zone of the Ti-48-2-2 substrate. Depletion of titanium and a possible low diffusion of niobium through the nitride layer resulted again in the precipitation of niobium rich intermetallic phases in the metal subsurface.

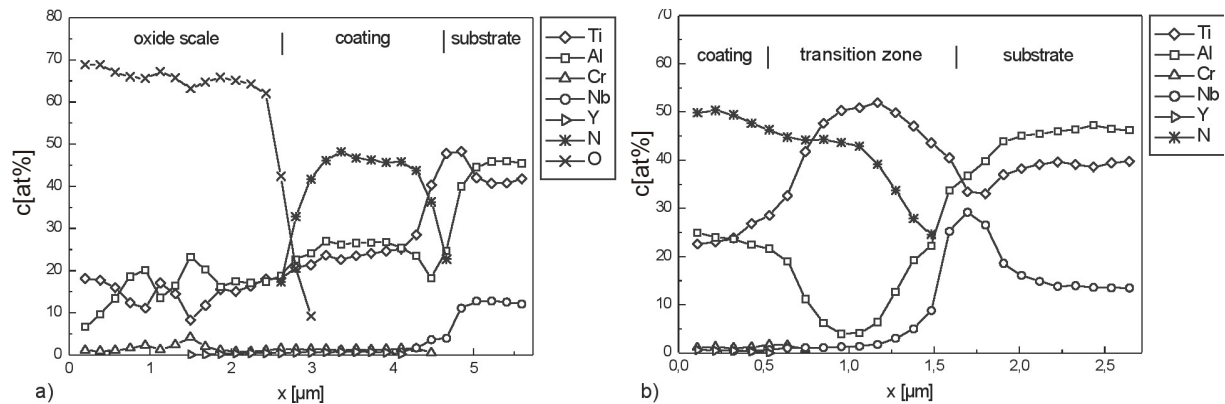


Figure 7: EDX analysis of Ti-45-8 specimen coated with nitride-1, which was oxidized 3000 h at 750°C, showing the concentration profiles across oxide scale, coating and substrate (a) as well as across the transition zone between nitride coating and substrate (b).

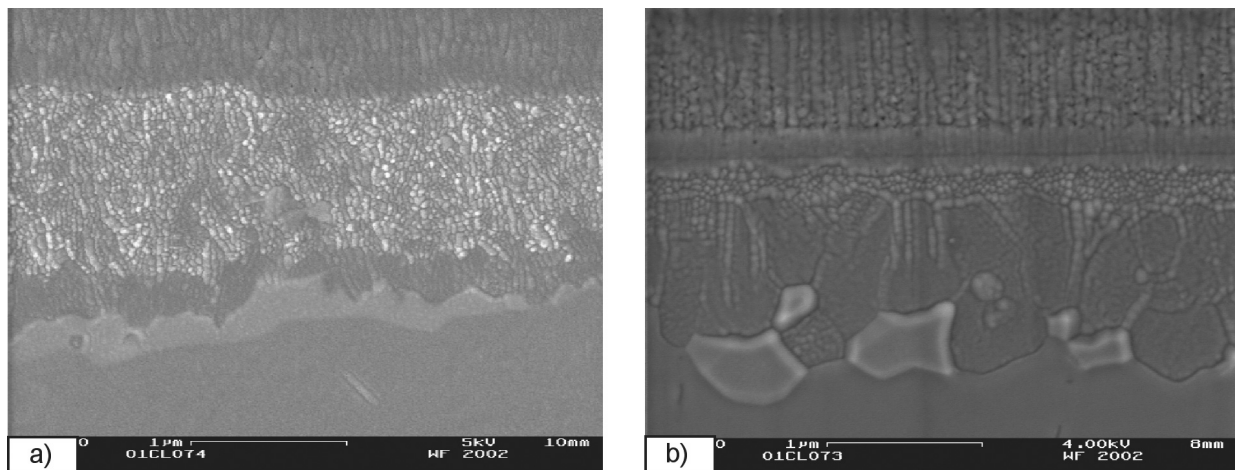


Figure 8. Scanning electron micrographs of Ti-45-8 (a) and Ti-48-2-2 (b) specimens coated with nitride-1, which were oxidized 3000 h at 750°C, showing the fine grained nitride layer of the transition zone.

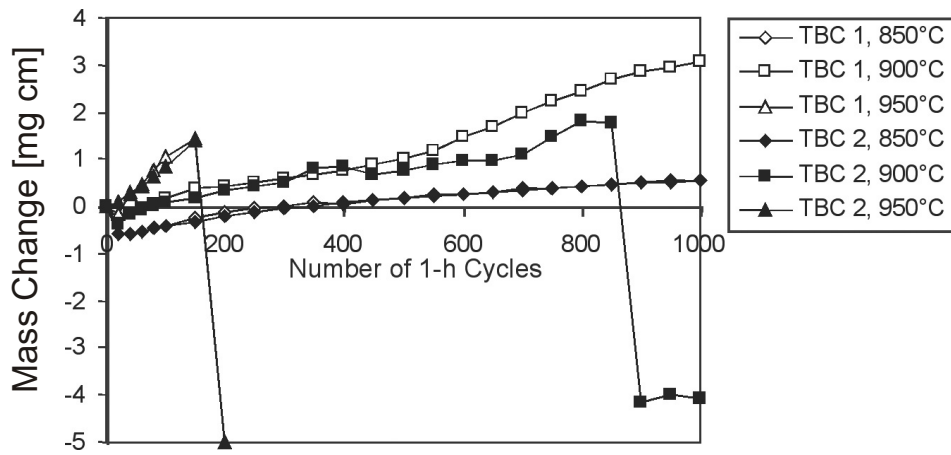


Figure 9: Performance of two different types of EB-PVD thermal barrier coatings on gamma titanium aluminide alloy Ti-45-8 between 850 and 950°C.

Performance of thermal barrier coatings on gamma TiAl

Cyclic oxidation tests between 850 and 950°C reveal a strong dependence upon temperature of the oxidation behavior and the resistance to spallation of the EB-PVD thermal barrier coatings on Ti-45-8 substrates (Fig. 9). Obviously, at 850°C, mass change due to oxidation was moderate, without any sign of oxide scale spallation. Notably, the initial weight loss of the specimens indicated in Fig. 9 was caused by the release of water during the first heating cycles (the specimens were weighed after 20 1-h cycles for the first time); the origin of the water was natural air humidity taken up by the specimens during storage before the tests were started. As

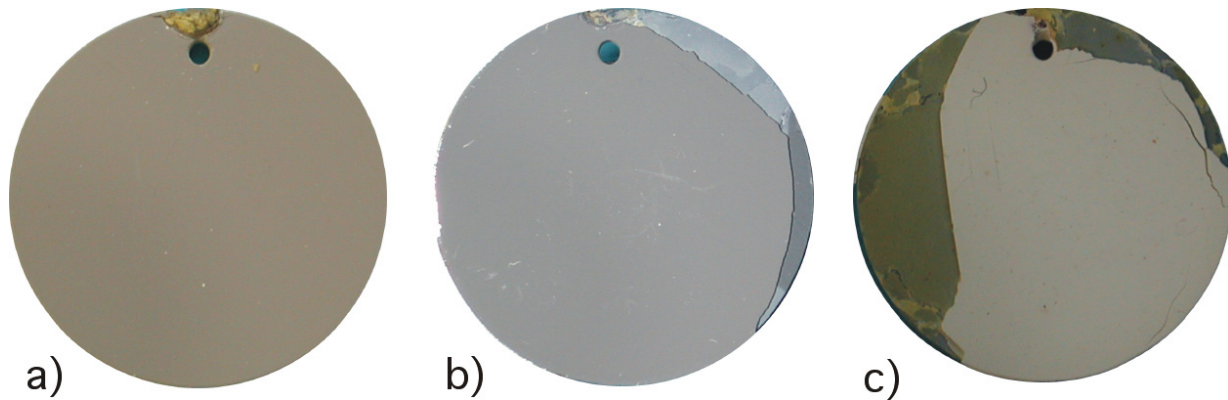


Figure 10: Photographs of TBC-2 specimens after cyclic oxidation. a) 850°C/1000h, b) 900°C/1000h, and 950°C/250h.

Fig. 10a demonstrates, the TBC was perfectly intact after 1000 1-h cycles at 850°C. The little bulb close to the hole of the specimen is the remainder of a specimen holder needed for coating deposition which had been removed before the oxidation test. In the case of 900°C exposure, TBC-2 started to spall partly after 850 1-h cycles. As Fig. 10b shows, spallation was initiated from the specimen edges, presumably starting from the area where the specimen holder was attached. Notably, spallation occurred only on one side of the specimen while the TBC on the backside was still intact. Despite of significant mass gain, TBC-1 was still intact when the tests were terminated after 1000 1-h cycles at 900°C. At 950°C rapid mass gain was measured for TBC-1 and TBC-2 caused by formation of a non-protective oxide scale underneath the thermal

barrier coating which was followed by spallation of the ceramic top coating that started after 150 1-h cycles. Spallation was again initiated from the edges of the specimens (Fig. 10c) and led to significant loss of the thermal barrier coating after 250 1-h cycles when the tests were terminated.

Post-oxidation scanning electron microscopy revealed that at all temperatures, as indicated by the mass changes from oxidation tests (Fig. 9), the pre-formed oxide scales were increased in thickness. Similar to the well-known failure modes of thermal barrier coatings on nickel-base alloys [11, 12], the failure of the ceramic coatings on gamma titanium aluminides occurs at the metal/thermally grown oxide scale interface or within the oxide scale, while the thermal barrier coating itself is well-adherent to the thermally grown oxide (Fig. 11). This mode of failure results in through-thickness loss of the ceramic top coating in the event of spalling. As indicated by Fig. 11 and confirmed by EDS analysis, the initially protective alumina scale cannot be maintained during high-temperature exposure. Instead a mixed alumina/titania oxide scale forms that grows fairly rapidly. Moreover, significant porosity within this growing oxide

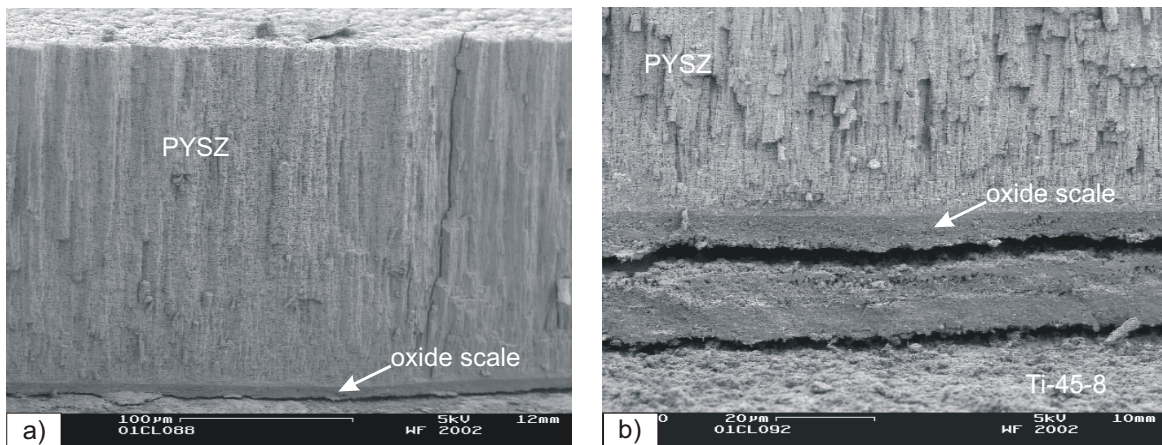


Figure 11: Typical failure location of an EB-PVD thermal barrier coating on Ti-45-8 after 250 1-h cycles at 950°C.

scale provides sites for crack initiation and pathways for crack propagation, thus promoting failure of the ceramic top layer. However, despite of a fairly thick oxide scale formed after 1000 1-h cycles at 850°C, the thermal barrier coating demonstrated very good adhesion.

Fig. 12a shows a scanning electron micrograph of a cross section of a specimen exposed at 850°C for 1000 1-h cycles. The oxide scale consisted of an outer layer of alumina with fine dispersed titania, a porous TiO_2 layer, and an interface oxide scale/substrate. Bonding between the thermal barrier coating and the oxide scale was sound. The growth front of the outer alumina layer was not straight but irregular. Titania was often found between the thermal barrier coating and the Al_2O_3 layer. In the porous TiO_2 layer, cracks were observed, demonstrating the weakness of this zone. Cracking might be associated with the preparation of the cross section, most probably resulting from sawing. Between the oxide scale and the substrate, a complex interface was formed. It was characterized by a discontinuous titanium nitride layer, interspersed with alumina particles, and an intermetallic phase enriched in niobium in the adjacent substrate (Fig. 12b). As supported by EDX analysis, the titanium nitride layer consisted of two nitrides, TiN and Ti_2AlN being formed adjacent to the oxide scale and substrate, respectively. Table 2 presents the composition of the different phases found in the interface oxide scale/substrate.

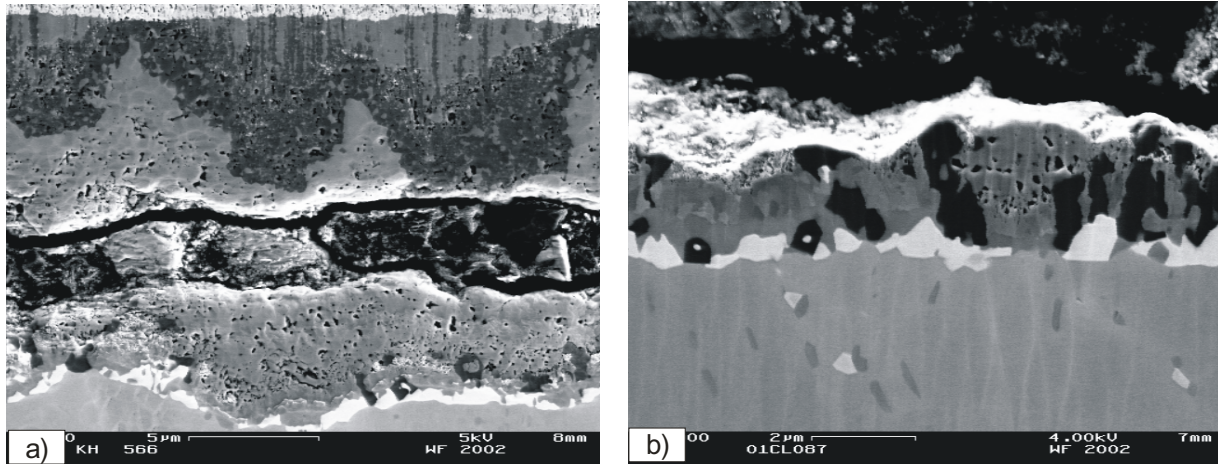


Figure 12: SEM micrograph of a specimen after 1000 1-h cycles at 850°C, showing the oxide scale (a) and the oxide/substrate interface (b).

Table 2. EDX analysis (at%) of different phases found at the interface oxide scale/substrate of a sample oxidized 1000h at 850°C.

	Ti	Al	Nb	O	N
nitride layer	44.0	18.8	3.3		33.9
dark phase	5.2	29.1	1.4	64.3	
bright phase	20.9	38.5	39.2		
matrix	47.6	42.0	10.4		

Fig. 13a shows concentration profiles of the relevant elements across the oxide scale of a specimen cycled at 850°C for 1000 h. Below the thermal barrier coating, a mixed oxide zone of Al_2O_3 and TiO_2 was found consisting predominantly of titania in the upper part and alumina in the lower part. Beneath this oxide mixture, a porous TiO_2 layer was formed containing a significant amount of niobium and a low content of aluminum. In the adjoining oxide scale/substrate interface nitrogen was detected. Concentration profiles across the interface taken at

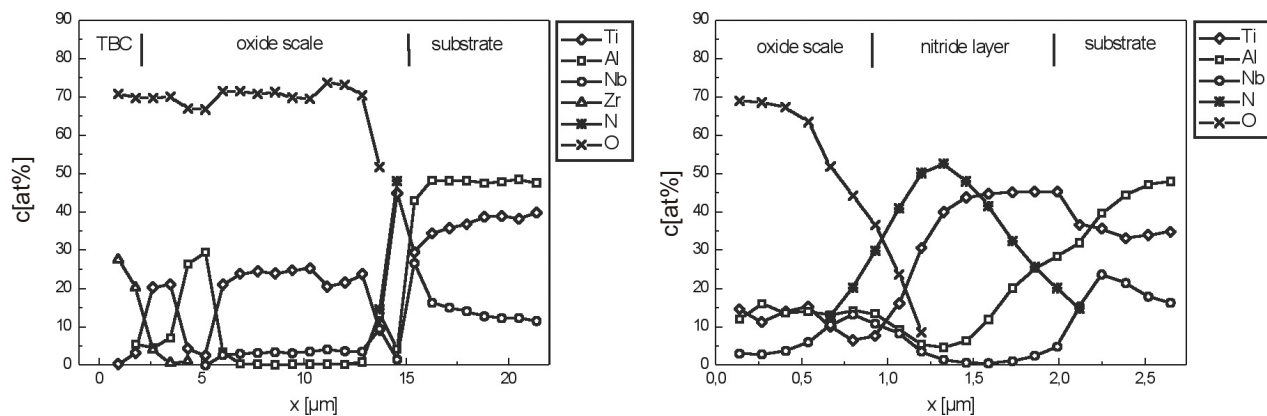


Figure 13: EDS analysis of a specimen after 1000 1-h cycles at 850°C, showing elemental profiles across the oxide scale (a) and the oxide/substrate interface (b).

higher resolution are plotted in Fig. 13b. Niobium enrichment was observed at both borderlines, oxide/nitride and nitride/substrate. Across the nitride layer the concentration of aluminum first decreased and then increased when approaching the substrate.

Fig. 14a shows a scanning electron micrograph of a specimen after 1000 1-h cycles at 900°C. The specimen failed in the porous TiO₂ layer. The oxide scale formed at the higher temperature exhibited a layered structure. Beneath the porous titania zone, wavy bright and dark bands were observed. The bright layer being porous was enriched in niobium, the dark layer consisted mainly of Al₂O₃ with interdispersed TiO₂ particles, as confirmed by EDX analysis. Compared to 800°C the density of alumina was increased at the oxide scale/substrate interface for specimens heated at 900°C. Al₂O₃ particles revealing an elongated shape were found adjacent to the niobium rich phase often including it (Fig. 14b). Therefore, this intermetallic phase enriched in niobium might stimulate the formation of alumina.

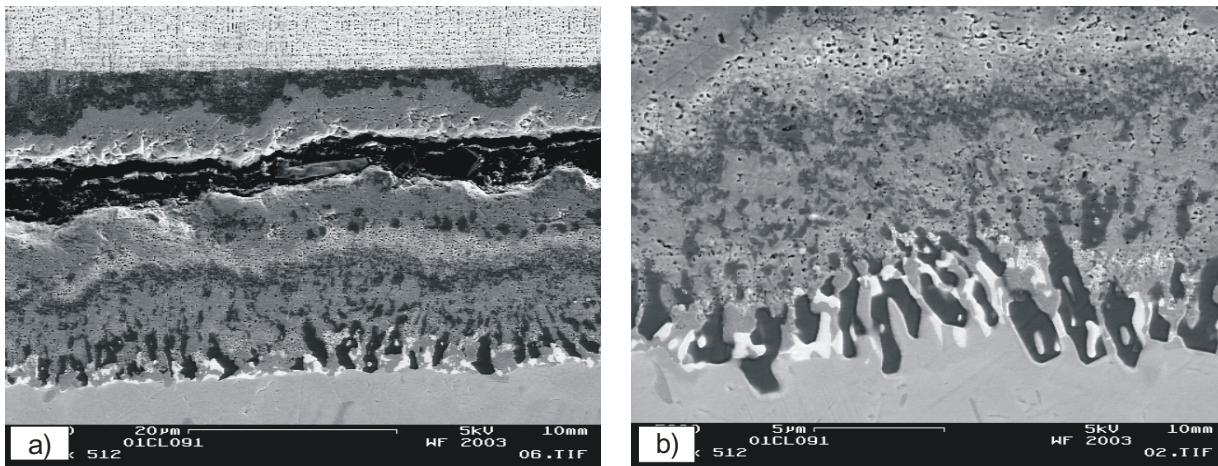


Figure 14: SEM micrograph of a specimen after 1000 1-h cycles at 900°C, showing the oxide scale (a) and the oxide/substrate interface (b).

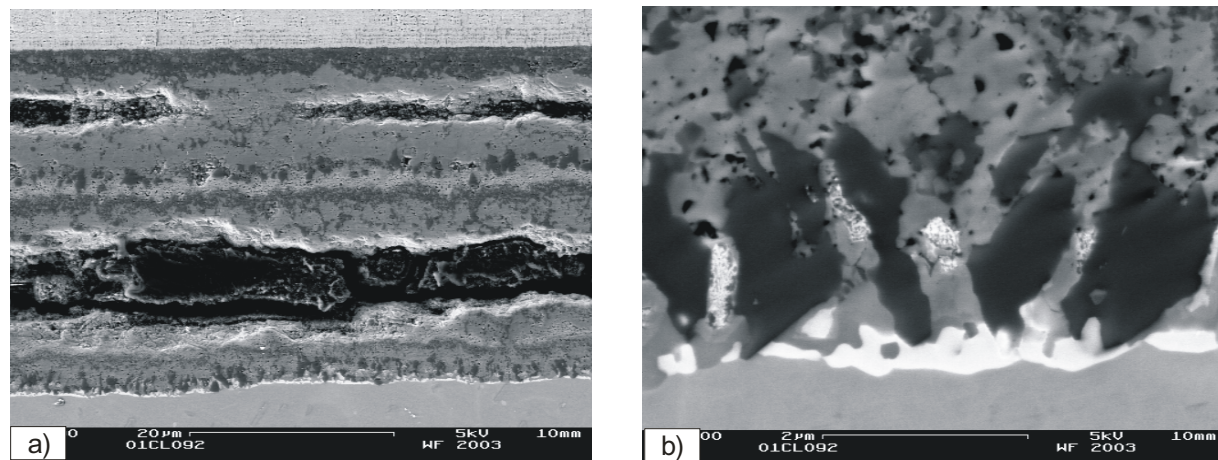


Figure 15: SEM micrograph of a specimen after 250 1-h cycles at 950°C, showing the oxide scale (a) and the oxide/substrate interface (b).

Fig. 15a shows a polished cross section of a specimen after 250 1-h cycles at 950°C. Two major crack paths were observed, predominantly in the porous TiO₂ layers. The oxide scale exhibited a pronounced layered structure. Broad porous titania layers were separated by a zone enriched in niobium, as corroborated by EDX analysis. This zone being also porous was bordered by

alumina rich bands being more dense at the lower side. The interface oxide scale/substrate is shown in Fig. 15b. The niobium rich precipitates at the upper side of the nitride layer were dissolved when buried in the growing oxide scale. Concentration profiles of the alloying elements in the metal subsurface zone are plotted in Fig. 16. Depletion of titanium was observed, whereas aluminium and niobium were enriched. Oxygen was not detected in the subsurface zone of γ -TiAl.

These promising initial results suggest that EB-PVD thermal barrier coatings may have the potential for long-term use at temperatures somewhat beyond 850°C. Clearly, oxidation of the substrate material is a major concern and limits the durability of the ceramic top coating. Therefore, oxidation resistant coatings that protect the substrate material from oxidation attack will be considered in this ongoing research effort. If surface temperatures of the order of 900°C would be acceptable for protected gamma titanium aluminides the use of thermal barrier coatings might enable replacement of heavy nickel-base alloys even in the hot section of aero engines.

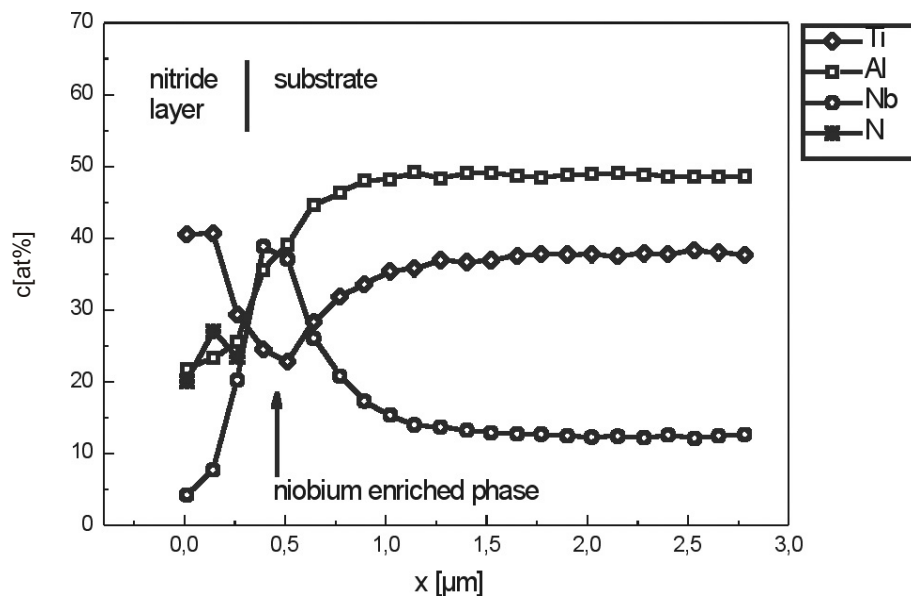


Figure 16: EDS analysis of a specimen after 250 1-h cycles at 950°C, showing transition between nitride layer and substrate.

Conclusions

Among the coatings tested, nitride coatings based on Ti-Al-Cr-Y-N, either monolithically grown or superlattice coatings, demonstrated excellent oxidation resistance at 750°C up to 3000 h under isothermal and cyclic conditions. During thermal exposure, nitride coatings formed protective oxide scales that further reduced environmental attack of the γ -TiAl base alloy. The nitride overlay coatings effectively prevented oxygen contamination of the base material while showing limited interaction with the alloy.

Although thermal barrier coatings on γ -TiAl substrate alloys are yet far away from technical application, initial results on EB-PVD partially yttria stabilized zirconia coatings deposited on Ti-45Al-8Nb are very promising. Without any oxidation protection thermal barrier coatings survived 1000 1-h cycles at 850°C with zero spallation. However, oxidation of the substrate limits the useful lifetime of these coatings, indicating that oxidation resistant intermediate coatings are necessary. Current research and development is directed towards improving the

high temperature capabilities of the nitride coatings presented in this study as well as other coatings to be used in thermal barrier coatings systems for γ -TiAl.

Acknowledgments

Ti-Al-Cr-Y-N coatings were provided by P.Eh. Hovsepian and W.-D. Münz (now at Techno Coat Oberflächentechnik, Germany) at Sheffield Hallam University, UK, which is gratefully acknowledged.

References

1. W. Smarlsy, H. Baur, G. Glitz, H. Clemens, T. Khan and M. Thomas, "Titanium aluminides for automotive and gas turbine applications", in *Structural Intermetallics 2001*, K.J. Hemker, *et al.*, Editors. 2001, TMS: Warrendale, PA. p. 25-34.
2. A. Gilchrist and T.M. Pollock, "Cast gamma titanium aluminides for low pressure turbine blades: a design case study for intermetallics", in *Structural Intermetallics 2001*, K.J. Hemker, *et al.*, Editors. 2001, TMS: Warrendale, PA. p. 3-12.
3. N.A. Walker and N.E. Glover, "Applications of intermetallics in the gas turbine", in *Structural Intermetallics 2001*, K.J. Hemker, *et al.*, Editors. 2001, TMS: Warrendale, PA. p. 19-24.
4. W.D. Münz, D. Schulze and F.J.M. Hauzer, *Surface and Coatings Technology*, 1992. **50**: p. 169.
5. I. Petrov, P. Losbichler, D. Bergstrom, J.E. Greene, W.D. Münz, T. Hurkmans and T. Trinh, *Thin Solid Films*, 1997. **302**: p. 179.
6. G. Håkansson, L. Hultman, J.E. Sundgren, J.E. Greene and W.D. Münz, *Surface and Coatings Technology*, 1991. **48**: p. 51.
7. C. Leyens, M. Peters, P.E. Hovsepian, D.B. Lewis, Q. Luo and W.-D. Münz, "Novel coating systems produced by the combined cathodic arc/unbalanced magnetron sputtering for environmental protection of titanium alloys". *Surface and Coatings Technology*, 2002. **155**(2-3): p. 103-111.
8. M.I. Lembke, D.B. Lewis, W.-D. Münz and J.M. Titchmarsh, "Significance of Y and Cr in TiAlN hard coatings for high speed cutting". *Surface Engineering*, 2001. **17**(2): p. 153-158.
9. C. Leyens, M. Peters and W.A. Kaysser, "Oxidation-resistant coatings for application on high-temperature titanium alloys in aeroengines". *Advanced Engineering Materials*, 2000. **2**(5): p. 265-269.
10. C. Leyens, J.-W. van Liere, M. Peters and W.A. Kaysser, "Magnetron-Sputtered Ti-Cr-Al Coatings for Oxidation Protection of Titanium Alloys". *Surface and Coatings Technology*, 1998. **108-109**: p. 30-35.
11. C. Leyens, U. Schulz, K. Fritscher, M. Bartsch, M. Peters and W.A. Kaysser, "Contemporary materials issues for advanced EB-PVD thermal barrier coatings". *Zeitschrift für Metallkunde*, 2001. **92**(7): p. 762-772.
12. C. Leyens, U. Schulz, B.A. Pint and I.G. Wright, "Influence of EB-PVD thermal barrier coating microstructure on thermal barrier coating system performance under cyclic oxidation conditions". *Surface and Coatings Technology*, 1999. **120-121**: p. 68-76.